Pure spin polarized transport based on Rashba spin–orbit interaction through the Aharonov–Bohm interferometer embodied four-quantum-dot ring*

Wu Li-Jun (吴丽君)[a)†] and Han Yu(韩 宇)[b)‡]

[a)] *School of Science, Shenyang Ligong University, Shenyang* 110159, *China*
[b)] *Department of Physics, Liaoning University, Shenyang* 110036, *China*

(Received 22 August 2012; revised manuscript received 9 October 2012)

The spin-polarized linear conductance spectrum and current–voltage characteristics in a four-quantum-dot ring embodied into Aharonov–Bohm (AB) interferometer are investigated theoretically by considering a local Rashba spin–orbit interaction. It shows that the spin-polarized linear conductance and the corresponding spin polarization are each a function of magnetic flux phase at zero bias voltage with a period of 2π, and that Hubbard U cannot influence the electron transport properties in this case. When adjusting appropriately the structural parameter of inter-dot coupling and dot-lead coupling strength, the electronic spin polarization can reach a maximum value. Furthermore, by adjusting the bias voltages applied to the leads, the spin-up and spin-down currents move in opposite directions and pure spin current exists in the configuration space in appropriate situations. Based on the numerical results, such a model can be applied to the design of a spin filter device.

Keywords: quantum dot ring, Rashba spin–orbit interaction, spin-polarized transport, "bound states in the continuum" phenomena, bias voltage, Aharonov–Bohm interferometer

PACS: 73.23.−b, 73.63.−b **DOI:** 10.1088/1674-1056/22/4/047302

1. Introduction

Generating and manipulating a spin-polarized current in semiconductor nanostructures has become one of the central subjects in the fields of mesoscopic physics and spintronics, and has aroused huge interest of researchers and the investigation of it has been extensively performed due to its relevance to quantum computation and quantum information.[1–3] The generation of spin-polarized current in spintronic devices is strongly desired.[4–9] Owing to the electron spin in a quantum dot (QD) serving as a natural candidate for the qubit, the QD has been regarded as an elementary cell of realizing solid state quantum computation, and much attention has been paid to the manipulation of the electron spin in the QD for its application in quantum devices. One must focus on how to efficiently polarize and manipulate the spin in the QD. One of the ideas is to couple the QD to a ferromagnetic (FM) lead, which is difficult to carry out because of the conductivity mismatch. An alternative method is to employ a magnetic field to polarize the spin in the QD, but one needs a very strong magnetic field confined to a small region of QD. In order to manipulate the electron spin efficiently, recently, an innovatory method of introducing a gradient electric field into the QD to induce the Rashba spin–orbit interaction (SOI) has been adopted. The Rashba spin–orbit interaction has been taken into consideration to avoid the usage of any magnetic material or field. It is a pure electrical method.

Spin–orbit (SO) coupling is an important mechanism that influences the spin state. The Rashba SOI is a kind of relativistic effect at the low-speed limit.[10–15] It arises from the inversion asymmetry of the electric field in a two-dimensional electron system. It can make its spin degree of freedom couple with orbital motion; spin-up and spin-down electrons traveling through the different Feynman paths will acquire different phases, resulting in an interesting spin-relevant phase coherence phenomenon, thus making it possible to control the electron spin in the external electric field or at gate voltage. The quantum-dot-ring has been fabricated and regarded as a candidate for manipulating electron spin. Recently, spin polarization and separation in triple or quadruple quantum-dot-rings have been put forward to take advantage of the SOI in such a geometry.[16–19] By applying a Rashba SO coupling to a QD locally, remarkable spin polarization comes about in the electron transport process through tuning the structure parameters, i.e., the magnetic flux or quantum dot levels. However, in the absence of magnetic flux, the spin polarization and spin separation can be simultaneously realized in such structures.[20–22]

In our previous work, the electron transport in N-QD ring embodied into an Aharonov–Bohm (AB) interferometer has been investigated,[23,24] and the results showed that the AB effect can provide more Feynman path of the electron coherent interference. The more decoupled states and antiresonance are present in the electronic transport through N-quantum-dot

*Project supported by the Natural Science Foundation of Liaoning Province, China (Grant No. 201202085), the National Natural Science Foundation of China (Grant No. 11004138), the Excellent Young Scientists Fund of Liaoning Provence, China (Grant No. LJQ2011020), and the Young Scientists Fund of Shenyang Ligong University (Grant No. 2011QN-04-11).

†Corresponding author. E-mail: wulijun20070915@163.com
‡Corresponding author. E-mail: hanyu@lnu.edu.cn

© 2013 Chinese Physical Society and IOP Publishing Ltd

ring embodied in the AB interferometer. The symmetry of the coupled-dot system and the magnetic flux through the AB interferometer are two physical mechanisms which lead to decoupled states. Even–odd parity oscillations occur in linear conductance spectra of such a highly symmetric quantum dot ring. Accordingly, it is desirable to investigate that in such a structure the electron spin transport behavior is controlled by the external field and the structure parameters.

As for the coupled-QD configurations, it is feasible to fabricate the QD rings including less than six dots in the current experiment. In this work, in terms of non-equilibrium Green function formalism,[25–27] we intend to investigate the behavior of both electronic spin-polarized conductance and spin-polarized current which is influenced by the structure parameters and the external field, and the current–voltage (J–v) characteristic driven by an infinite bias in a four-quantum-dot ring embedded in the AB interferometer. The four-quantum-dot ring is the smallest element which possesses the symmetry of structure. The numerical results indicate that when an appropriate magnetic field is applied, the spin polarization in such a configuration can reach as high as 100%. Furthermore, by adjusting the bias voltage applied to the leads, the spin-up and spin-down current can be moved in opposite directions and pure spin current exists in the configuration space in appropriate situations. Simultaneously, the intra-dot Coulomb interaction is considered.

The rest of the present paper is organized as follows. In Section 2 the model Hamiltonian and theoretical formalism are presented. In Section 3 molecular orbital representation is explicated. In Section 4 the numerical results and discussion are given. Finally, some conclusions drawn from the present study are summarized in Section 5.

2. Model and formulation

The structure of a coupled QD ring system that is to be considered is illustrated in Fig. 1. A four-quantum-dot ring is embedded into the AB interferometer symmetrically. A magnetic flux threads through the AB ring and a Rashbar spin–orbit interaction only exists in the QD-1 (shaded one) embedded into one arm of the AB interferometer. Rashba SOI induces a spin-dependent phase factor in the electron tunneling function. The left (L) and right (R) leads possess the electrical chemical potentials $\mu_{\rm L}$ and $\mu_{\rm R}$, respectively. A symmetric bias voltage v applied to two leads results in the chemical potential difference so that $\mu_{\rm L} = -\mu_{\rm R} = v/2$. Intra-dot Coulomb interaction U is taken into account when inter-dot Coulomb interaction among electrons is neglected. The electronic motion of system can be described by the following Hamiltonian H:

$$H = H_{\rm C} + H_{\rm D} + H_{\rm T}, \tag{1}$$

where $H_{\rm C}$ is the Hamiltonian for the non-interacting electrons in the left and right leads,

$$H_{\rm C} = \sum_{\sigma k\alpha\in {\rm L,R}} \varepsilon_{\alpha k} c^{\dagger}_{\alpha k\sigma} c_{\alpha k\sigma},$$

$H_{\rm D}$ describes the local electron in the four-quantum-dot ring,

$$H_{\rm D} = \sum_{\sigma j=1}^{4} \varepsilon_j d^{\dagger}_{j\sigma} d_{j\sigma} + (t_4 d^{\dagger}_{4\sigma} d_{1\sigma} + \sum_{j=1}^{3} t_j d^{\dagger}_{j\sigma} d_{j+1\sigma} + {\rm h.c.}) + \sum_{j=1}^{4} U_j n_{j\uparrow} n_{j\downarrow},$$

and $H_{\rm T}$ denotes the electron tunneling between the leads and the quantum dots,

$$H_{\rm T} = \sum_{\sigma k\alpha\in L,R} (V_{1\alpha\sigma} d^{\dagger}_{1\sigma} c_{\alpha k\sigma} + V_{3\alpha\sigma} d^{\dagger}_{3\sigma} c_{\alpha k\sigma}) + {\rm h.c.} \tag{2}$$

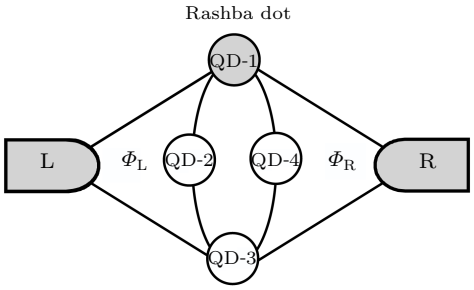


Fig. 1. Schematic plot of a four-QD ring embodied in an Aharonov–Bohm interferometer with a local Rashbar spin–orbit interaction applied to the QD-1.

In the above Hamiltonians, $c^{\dagger}_{\alpha k\sigma}$ and $d^{\dagger}_{j\sigma}$ ($c_{\alpha k\sigma}$ and $d_{j\sigma}$) are the operators to create (annihilate) the electron of the continuous state $|k_\alpha,\sigma\rangle$ in the lead-α and the electron in QD-j with spin $\sigma =\uparrow,\downarrow$ ($\sigma = \pm 1$), respectively; $\varepsilon_{k\alpha}$ and ε_j denote the corresponding single-particle energy levels; t_j ($j = 1,2,3,4$) is the inter-dot tunneling coupling coefficient between the QD-j and QD-(j+1) (when $j = 4$, $j+1 \Rightarrow 1$), which can be tuned by the gate voltage; U_j is the intra-dot Coulomb repulsion with $n_{j\sigma} = d^{\dagger}_{j\sigma} d_{j\sigma}$ being the particle number operator; $V_{j\alpha\sigma}$ ($j = 1,3$) is the tunneling coupling strength between QD-j and lead-α. The tunneling matrix elements take the following values $V_{1{\rm L}\sigma} = V_{\rm L}\,{\rm e}^{{\rm i}((\phi_{\rm L}/2)-\sigma\varphi)}$, $V_{3{\rm L}\sigma} = V_{\rm L}\,{\rm e}^{-{\rm i}(\phi_{\rm L}/2)}$, $V_{1{\rm R}\sigma} = V_{\rm R}\,{\rm e}^{-{\rm i}((\phi_{\rm R}/2)-\sigma\varphi)}$, and $V_{3{\rm R}\sigma} = V_{\rm R}\,{\rm e}^{{\rm i}(\phi_{\rm R}/2)}$. We assume $V_{\rm L} = V_{\rm R} = V$ to be constants in the following calculation. $\phi_{\rm L}$ and $\phi_{\rm R}$ arise from the magnetic flux Φ threading through the AB interferometer, in which $\phi_\alpha = 2\pi\Phi/\Phi_0$ with the flux quantum $\Phi_0 = hc/e$, describes the magnetic flux induced phase factor. The spin-dependent phase factor φ is associated with the Rashba SOI coupling on QD-1, which arises from the Rashba-induced spin precession in the electron traveling process.

The quantum transport property of this device is analyzed by using the nonequilibrium Green's function technique. When Rashba interaction comes into play, the current flowing from the left lead into the ring becomes spin-dependent on the index σ, and it can be calculated from the time evolution of the occupation number for electrons in the left lead, which is written as

$$J_{\rm L} = -e\left\langle \dot{N}_{\rm L} \right\rangle = \frac{{\rm i}e}{\hbar}[N_{\rm L}, H], \tag{3}$$

where $N_{\rm L}=\sum_{k\sigma}c^{\dagger}_{{\rm L}k\sigma}c_{{\rm L}k\sigma}$ is the particle number operator in lead-L. Then we can obtain the formula of the spin-dependent current in lead-L as follows:

$$J_{{\rm L}\sigma}=\frac{{\rm i}e}{\hbar}\sum_{k}[V_{kL,j}\langle c^{\dagger}_{{\rm L}k\sigma}d_{j\sigma}\rangle-V^{*}_{kL,j}\langle d^{\dagger}_{j\sigma}c_{{\rm L}k\sigma}\rangle]. \tag{4}$$

The lesser Green's function can be defined as follows:

$$\boldsymbol{G}^{<}_{j,{\rm L}k\sigma}(t,t')\equiv{\rm i}\langle c^{\dagger}_{{\rm L}k\sigma}(t')d_{j\sigma}(t)\rangle,$$

$$\boldsymbol{G}^{<}_{{\rm L}k\sigma,j}(t,t')\equiv{\rm i}\langle d^{\dagger}_{j\sigma}(t')c_{{\rm L}k\sigma}(t)\rangle.$$

Their relationship can be expressed as $\boldsymbol{G}^{<}_{{\rm L}k\sigma,j}(t,t')=-[\boldsymbol{G}^{<}_{j,{\rm L}k\sigma}(t,t')]^{*}$. Equation (4) is written as

$$J_{{\rm L}\sigma}=\frac{2e}{\hbar}{\rm Re}\Big\{\sum_{k}V_{k{\rm L}\sigma,j}\boldsymbol{G}^{<}_{j,{\rm L}k\sigma}(t,t')\Big\}. \tag{5}$$

The lesser Green's function $\boldsymbol{G}^{<}_{j,{\rm L}k\sigma}(t,t')$ can be obtained directly from the Langreth theory as

$$\boldsymbol{G}^{<}_{j,{\rm L}k\sigma}(t,t')=\sum_{j'}\int{\rm d}t_1V^{*}_{kL,j'}\big[\boldsymbol{G}^{\rm r}_{jj',\sigma}(t,t')g^{<}_{{\rm L}k}(t,t')+\boldsymbol{G}^{<}_{jj',\sigma}(t,t')g^{\rm a}_{{\rm L}k}(t,t')\big]. \tag{6}$$

In the above equations and hereafter, $\boldsymbol{G}^{{\rm r,a},<}_{jj',\sigma}(t,t')$ are the retarded, advanced, and lesser Green's functions of the QD defined as

$$\boldsymbol{G}^{\rm r}_{jj',\sigma}(t,t')=-{\rm i}\theta(t-t')\langle\{d_{j\sigma}(t),d^{\dagger}_{j'\sigma}(t')\}\rangle,$$

$$\boldsymbol{G}^{\rm a}_{jj',\sigma}(t,t')={\rm i}\theta(t'-t)\langle\{d_{j\sigma}(t),d^{\dagger}_{j'\sigma}(t')\}\rangle,$$

$$\boldsymbol{G}^{<}_{jj',\sigma}(t,t')={\rm i}\langle d^{\dagger}_{j'\sigma}(t'),d_{j\sigma}(t)\rangle;$$

the Fourier transform is $\boldsymbol{G}^{{\rm r,a},<}_{jj',\sigma}(\varepsilon)$ with the relationship $G^{{\rm r,a},<}_{\sigma}(\varepsilon)=\int G^{{\rm r,a},<}_{\sigma}(t)\,{\rm e}^{{\rm i}\varepsilon t}\,{\rm d}t$; $g^{{\rm r,a},<}_{{\rm L}k}(t,t')$ is the corresponding Green's function of the freedom electron in the lead-L. The Fourier transform of Eq. (6) is written as

$$\boldsymbol{G}^{<}_{j,{\rm L}k\sigma}(\varepsilon)=\sum_{j'\sigma}V^{*}_{k{\rm L}\sigma,j'}[\boldsymbol{G}^{\rm r}_{jj',\sigma}(\varepsilon)g^{<}_{{\rm L}k}(\varepsilon)+\boldsymbol{G}^{<}_{jj',\sigma}(\varepsilon)g^{\rm a}_{{\rm L}k}(\varepsilon)], \tag{7}$$

where $g^{<}_{{\rm L}k}(\varepsilon)=2\pi{\rm i}f_{\rm L}(\varepsilon)\delta(\varepsilon-\varepsilon_{{\rm L}k})$, $g^{\rm a}_{{\rm L}k}(\varepsilon)-g^{\rm r}_{{\rm L}k}(\varepsilon)=2\pi{\rm i}\delta(\varepsilon-\varepsilon_{{\rm L}k})$. Equation (5) can be expressed as

$$\begin{aligned}J_{{\rm L}\sigma}&=\frac{2e}{\hbar}\int\frac{{\rm d}\varepsilon}{2\pi}{\rm Re}\{\sum_{jj'k}V_{k{\rm L}\sigma,j}V^{*}_{k{\rm L}\sigma,j'}[\boldsymbol{G}^{\rm r}_{jj',\sigma}(\varepsilon)g^{<}_{{\rm L}k}(\varepsilon)+\boldsymbol{G}^{<}_{jj',\sigma}(\varepsilon)g^{\rm r}_{{\rm L}k}(\varepsilon)]\}\\&=\frac{{\rm i}e}{\hbar}\int\frac{{\rm d}\varepsilon}{2\pi}{\rm Tr}\Big(\Gamma^{\rm L}_{\sigma}(\varepsilon)\Big\{\boldsymbol{G}^{<}_{\sigma}(\varepsilon)+f_{\rm L}(\varepsilon)[\boldsymbol{G}^{\rm r}_{\sigma}(\varepsilon)-\boldsymbol{G}^{\rm a}_{\sigma}(\varepsilon)]\Big\}\Big),\end{aligned} \tag{8}$$

where $f_{\rm L}(\varepsilon)=[1+\exp(\varepsilon-\mu_{\rm L})/k_{\rm B}T]^{-1}$ is the Fermi distribution function of the lead-L,

$$[\Gamma^{\rm L}_{\sigma}(\varepsilon)]_{jj'}=2\pi\rho_{{\rm L}\sigma}(\varepsilon_{{\rm L}k})V_{k{\rm L}\sigma,j}(\varepsilon_{{\rm L}k})V^{*}_{k{\rm L}\sigma,j'}(\varepsilon_{{\rm L}k})$$

is the coupling between the QDs and the lead-L with $\rho_{{\rm L}\sigma}(\varepsilon_{{\rm L}k})$ being the spin-dependent density of the lead-L electrons, which is regarded as a constant since the electron reservoir usually consists of two-dimensional free electron gas. Using the same method, we can obtain the corresponding formula of the spin-dependent current through the lead-R:

$$J_{{\rm R}\sigma}=\frac{{\rm i}e}{\hbar}\int\frac{{\rm d}\varepsilon}{2\pi}{\rm Tr}\Big(\Gamma^{\rm R}_{\sigma}(\varepsilon)\big\{G^{<}_{\sigma}(\varepsilon)+f_{\rm R}(\varepsilon)\big[\boldsymbol{G}^{\rm r}_{\sigma}(\varepsilon)-\boldsymbol{G}^{\rm a}_{\sigma}(\varepsilon)\big]\big\}\Big),$$

and the spin-dependent current through the whole system can be given as follows:

$$J_{\sigma}=\frac{J_{{\rm L}\sigma}-J_{{\rm R}\sigma}}{2}=\frac{{\rm i}e}{2\hbar}\int\frac{{\rm d}\varepsilon}{2\pi}{\rm Tr}\Big\{[\Gamma^{\rm L}_{\sigma}(\varepsilon)-\Gamma^{\rm R}_{\sigma}(\varepsilon)]\boldsymbol{G}^{<}_{\sigma}(\varepsilon)+[f_{\rm L}(\varepsilon)\Gamma^{\rm L}_{\sigma}(\varepsilon)-f_{\rm R}(\varepsilon)\Gamma^{\rm R}_{\sigma}(\varepsilon)][\boldsymbol{G}^{\rm r}_{\sigma}(\varepsilon)-\boldsymbol{G}^{\rm a}_{\sigma}(\varepsilon)]\Big\}. \tag{9}$$

We use the Dyson equation of motion to calculate the retarded (advanced) Green's functions and adopt the Hubbard-II approximation to truncate the higher order Green's function. The results from such an approach are that the influence of electron correlation interaction on the transport properties, such as Kondo effect, is left out. When the electron interaction in the QD is not very strong and QD levels are not much lower than the Fermi energy, this approximation is a reasonable approximation. We can obtain the lesser Green's function $\boldsymbol{G}^{<}_{\sigma}(\varepsilon)$ with the Keldysh equation, $\boldsymbol{G}^{<}_{\sigma}(\varepsilon)=\boldsymbol{G}^{\rm r}_{\sigma}(\varepsilon)\boldsymbol{\Sigma}^{<}_{\sigma}(\varepsilon)\boldsymbol{G}^{\rm a}_{\sigma}(\varepsilon)$, in which the lesser self-energy is $\boldsymbol{\Sigma}^{<}_{\sigma}(\varepsilon)={\rm i}(f_{\rm L}(\varepsilon)\boldsymbol{\Gamma}^{\rm L}_{\sigma}+f_{\rm R}(\varepsilon)\boldsymbol{\Gamma}^{\rm R}_{\sigma})$. Formula (9) can be written as

$$J_{\sigma}=\frac{e}{h}\int{\rm d}\varepsilon T_{\sigma}(\varepsilon)[f_{\rm L}(\varepsilon)-f_{\rm R}(\varepsilon)], \tag{10}$$

with spin-dependent transmission probability

$$T_{\sigma}(\varepsilon)={\rm Tr}\big\{\boldsymbol{G}^{\rm a}_{\sigma}(\varepsilon)\boldsymbol{\Gamma}^{\rm R}_{\sigma}\boldsymbol{G}^{\rm r}_{\sigma}(\varepsilon)\boldsymbol{\Gamma}^{\rm L}_{\sigma}\big\}. \tag{11}$$

The above equation is a well-known Landaur–Büttiker current formula for mesoscopic systems. When the electron transport is in the linear regime, the spin-dependent linear conductance $\mathcal{G}_{\sigma}$ at zero bias and low-temperature limit can be obtained as

$$\mathcal{G}_{\sigma}=\frac{e^2}{h}T_{\sigma}(\varepsilon)|_{\varepsilon=\varepsilon_{\rm F}}, \tag{12}$$

and the retarded (advanced) Green's functions ($\boldsymbol{G}^{\rm a}_{\sigma}(\varepsilon)=[\boldsymbol{G}^{\rm r}_{\sigma}(\varepsilon)]^{\dagger}$) in a matrix form are

$$\boldsymbol{G}^{\rm r}_{\sigma}(\varepsilon)=\{[g^{\rm r}_{\sigma}(\varepsilon)]^{-1}-\boldsymbol{\Sigma}^{\rm r}_{T\sigma}(\varepsilon)\}^{-1}, \tag{13}$$

where

$$[g^{\rm r}_{\sigma}(\varepsilon)]^{-1}=\begin{bmatrix}(z-\varepsilon_1)S_{1\sigma} & -t_1 & 0 & -t^{*}_4\\ -t^{*}_1 & (z-\varepsilon_2)S_{2\sigma} & -t_2 & 0\\ 0 & -t^{*}_2 & (z-\varepsilon_3)S_{3\sigma} & -t_3\\ -t_4 & 0 & -t^{*}_3 & (z-\varepsilon_4)S_{4\sigma}\end{bmatrix}, \tag{14}$$

$$\Sigma^{\rm r}_{T\sigma}(\varepsilon) = -\frac{\rm i}{2}(\Gamma^{\rm L}_{\sigma} + \Gamma^{\rm R}_{\sigma}), \tag{15}$$

$$\Gamma^{\rm L(R)}_{\sigma} = \begin{bmatrix} \Gamma^{\rm L(R)}_{11} & 0 & \sqrt{\Gamma^{\rm L(R)}_{11}\Gamma^{\rm L(R)}_{22}}\,{\rm e}^{\pm {\rm i}(\phi_{\rm L(R)} - \sigma\varphi)} & 0 \\ 0 & 0 & 0 & 0 \\ \sqrt{\Gamma^{\rm L(R)}_{11}\Gamma^{\rm L(R)}_{22}}\,{\rm e}^{\mp {\rm i}(\phi_{\rm L(R)} - \sigma\varphi)} & 0 & \Gamma^{\rm L(R)}_{22} & 0 \\ 0 & 0 & 0 & 0 \end{bmatrix}. \tag{16}$$

In the above expression, $g^{\rm r}_{\sigma}(\varepsilon)$ is the retarded Green's function of the isolated four-QD system for the case where the inter-dot coupling coefficient is t_j in the absence of Rashba interaction with $z = \varepsilon + {\rm i}0^+$, and

$$S_{j\sigma} = \frac{z - \varepsilon_j - U_j}{z - \varepsilon_j - U_j + U_j\langle n_{j\bar{\sigma}}\rangle}$$

accounts for the effect of electron intra-dot Coulomb interaction within the second-order truncated approximation (SOA) method of the motion of the Green?s functions.[28] Besides, the spin-σ average electron occupation numbers in QD-j, $\langle n_{j\sigma}\rangle$, at zero temperature approximation is given by $\langle n_{j\sigma}\rangle = -\frac{1}{\pi}\int {\rm d}\varepsilon {\rm Im}\boldsymbol{G}^{\rm r}_{j\sigma,j\sigma}(\varepsilon)$. So the Green?s function can be solved by numerical iteration technique.

3. Molecular orbital representation

For the noninteracting case, the linear conductance spectra of the coupled QD structure reflect the eigenenergy spectra of the "molecules" made up of the coupled QDs. In other words, each resonant peak in the conductance spectra represents an eigenenergy of the total QD molecules, rather than the levels of the individual QDs. Therefore, it is necessary to transform the Hamiltonian into the molecular orbital representation of the QDs. It is quite helpful to analyze the numerical results for the linear conductance spectra.

We then introduce the electron creation (annihilation) operators corresponding to the molecular orbits, i.e. $f^{\dagger}_{m\sigma}$ ($f_{m\sigma}$). By diagonalizing the single-particle Hamiltonian of the QDs, we find the relation between the molecular and atomic representations (here, each QD is regarded as an "atom"), which is expressed as $[f^{\dagger}_{\sigma}] = [\eta][d^{\dagger}_{\sigma}]$. The transfer matrix $[\eta]$ consists of the eigenvectors of the QD Hamiltonian. In the molecular orbital representation, the single-particle Hamiltonian takes the form

$$H = \sum_{k\sigma\alpha\in L,R}\varepsilon_{\alpha k}c^{\dagger}_{\alpha k\sigma}c_{\alpha k\sigma} + \sum_{m=1,\sigma}^{4} e_m f^{\dagger}_{m\sigma}f_{m\sigma} + \sum_{\alpha k\sigma,m=1}^{4} v_{\alpha m\sigma}f^{\dagger}_{m\sigma}c_{\alpha k\sigma} + {\rm h.c.},$$

in which e_m is the eigenenergy of the QD molecules given by $e_m = \varepsilon_j + 2t_j\cos(m\pi/2)$; $v_{\alpha m\sigma} = V_{\alpha j\sigma}[\eta]^{\dagger}_{jm} + V_{\alpha j'\sigma}[\eta]^{\dagger}_{j'm}$ denotes the coupling between molecular state $|m,\sigma\rangle$ and state $|k,\sigma\rangle$ in lead-α. In the symmetric case the above relation can be rewritten as

$$v_{{\rm L(R})m\sigma} = V\,{\rm e}^{\pm {\rm i}\left((\phi_{\rm L(R)}/2) - \sigma\varphi\right)}\left([\eta]^{\dagger}_{jm} + [\eta]^{\dagger}_{j'm}\,{\rm e}^{\mp {\rm i}(\phi_{\rm L(R)} - \sigma\varphi)}\right),$$

with

$$[\eta] = \sqrt{\frac{1}{4}}\begin{bmatrix} {\rm i} & -1 & -{\rm i} & 1 \\ -1 & 1 & -1 & 1 \\ -{\rm i} & -1 & {\rm i} & 1 \\ 1 & 1 & 1 & 1 \end{bmatrix}.$$

We here define $\gamma^{\alpha}_{mm\sigma} = 2\pi v_{\alpha m\sigma}v^{*}_{\alpha m\sigma}\rho_{\alpha\sigma}(\varepsilon)$, which denotes the strength of the coupling between molecular state $|m,\sigma\rangle$ and state $|k,\sigma\rangle$ in lead-α. We also can rewrite $\gamma^{\alpha}_{mm\sigma}$ as

$$\gamma^{\rm L(R)}_{mm,\sigma} = \Gamma|[\eta]^{\dagger}_{jm} + [\eta]^{\dagger}_{j'm}\,{\rm e}^{\mp {\rm i}(\phi_{\rm L(R)} - \sigma\varphi)}|^2, \tag{17}$$

where $\Gamma = 2\pi V^2\rho_{\alpha}(\omega)$. If the value of $\gamma^{\alpha}_{mm\sigma}$ is equal to zero, it means that the molecular state $|m,\sigma\rangle$ will be decoupled from the lead-α completely, which induces the occurrence of "bound states in the continuum" (BIC). The molecular state $|m,\sigma\rangle$ becomes a bound state.[22]

4. Numerical results and discussion

With the solution of Green's function given in Section 2, we can perform a numerical calculation to show the characteristics of the linear conductance and current. When Rashba interaction comes into play, the conductance and current are spin-dependent on index σ. The charge current $J_{\rm C}$ and the spin current $J_{\rm S}$ are respectively defined as $J_{\rm C} = J_{\uparrow} + J_{\downarrow}$ and $J_{\rm S} = J_{\uparrow} - J_{\downarrow}$, and the corresponding polarization is $P_J = (J_{\uparrow} - J_{\downarrow})/(J_{\uparrow} + J_{\downarrow})$. In the linear regime, the spin polarization of the conduction is defined as $p = (\mathcal{G}_{\uparrow} - \mathcal{G}_{\downarrow})/(\mathcal{G}_{\uparrow} + \mathcal{G}_{\downarrow})$.[23] For simplifying the calculation, we consider the case of symmetric coupling between QDs and leads, and all energy and coupling strengths are measured in units of t_0, which is the unit of energy throughout this paper. We also take the Fermi level $\varepsilon_{\rm F}$ as the zero point of energy.

Figures 2(a)–2(d) show the spin-polarized linear conductance and the spin polarization each as a function of magnetic flux phase ϕ for different values of Γ, t_j, and φ with $\varepsilon_j = 0$, $\varepsilon_{\rm F} = 0$ at zero bias voltage. Hubbard U cannot influence the electron transport properties as a result of the electron interaction formula $(z - \varepsilon_j)S_{j\sigma}$ with $\varepsilon_j = 0$, $\varepsilon_{\rm F} = 0$ in this case. Figure 2(a) shows that the linear conductance of each spin component is the periodic function of ϕ with a period of 2π for $\varphi = \pi/2$ and $\Gamma = t_j = t_0$. When ϕ approaches $\phi = (4n+3)\pi/2$ ($n \in$ integer), the spin-up conductance $\mathcal{G}_{\uparrow}$ reaches its maximum value (solid line), while the spin-down conductance $\mathcal{G}_{\downarrow}$ becomes exactly zero (dashed line). It means that by adjusting the magnetic flux ϕ, a completed spin-polarized conductance can be driven in the device. The opposite behavior happens at $\phi = (4n+1)\pi/2$, when the spin-down conductance arrives at

a maximum value, the spin-up conductance is zero. Now the spin polarization $p=(\mathcal{G}_\uparrow-\mathcal{G}_\downarrow)/(\mathcal{G}_\uparrow+\mathcal{G}_\downarrow)=-1$. So the sign of the spin polarization can also be tuned over by tuning of the magnetic flux ϕ as shown in Fig. 2(b) by the solid line with the same parameters. These results can be explained directly by the following spin-dependent transmission probability:

$$T_\sigma(z) = 4\Gamma_0^2\frac{(z-\varepsilon_0)^2}{|\det(A)|^2}\Big|\cos(\phi-\sigma\varphi)(z-\varepsilon_0)^2 + 2t_0^2\big[1-\cos(\phi-\sigma\varphi)\big]\Big|^2, \tag{18}$$

where

$$\det(A)=\Big[(z-\varepsilon_0)^2+2\mathrm{i}\Gamma_0(z-\varepsilon_0)-\Gamma_0^2\sin^2(\phi-\sigma\varphi)\Big](z-\varepsilon_0)^2$$

and $z=\varepsilon_\mathrm{F}+\mathrm{i}0^+$, which is obtained by Eqs. (11)–(16). Therefore, for $\phi=(2n+1)\pi+\sigma\varphi$, T_σ has a maximum value, while $\phi=2n\pi+\sigma\varphi$, T_σ is zero. The maximum value of $T_\uparrow$ is corresponding to the zero of $T_\downarrow$ at the position of $\phi=(4n+3)\pi/2$ for $\varphi=\pi/2$. Figures 2(b) and 2(c) (dashed line) show $T_\uparrow$, $T_\downarrow$, and p for $\varphi=\pi/4$, which are also easily understood by Eq. (18). As a result of this fact, we can fully control $\pm100\%$ spin polarization at zero bias by adjusting the matching of ϕ and φ. It indicates that the magnetic flux ϕ and Rashba SOI phases factor φ can modulate the Feynman path interference when the electrons transport through the system. The Rashba SOI can be considered to be the essential cause for the spin-polarized behavior of the electron transport, in that the spin-polarized phenomenon vanishes at $\varphi=0$, which is shown in Fig. 2(c) (dotted line). Meanwhile, we find that the resonance-peak becomes sharper for weak coupling strengths of inter-dot and lead-dot with $t_j=0.1t_0$ and $\Gamma=0.1t_0$, respectively, shown in Fig. 2(d).

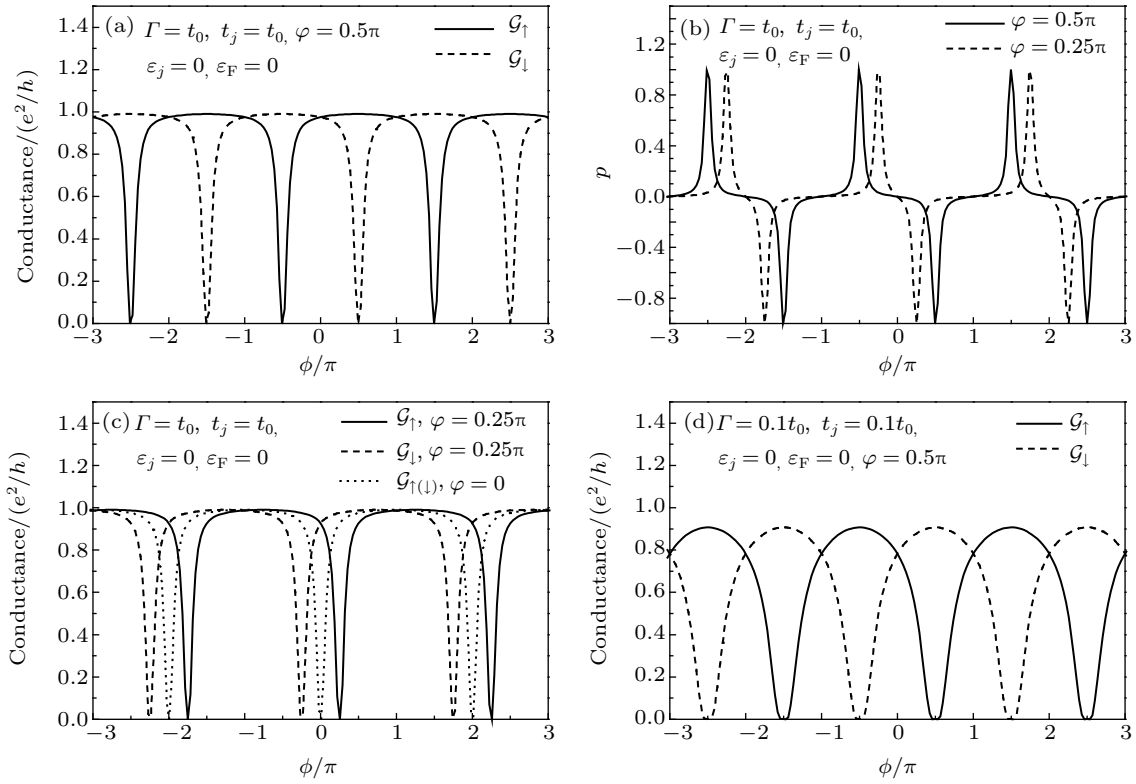


Fig. 2. ((a), (c), and (d)) spin-up conductance $\mathcal{G}_\uparrow$ (solid line) and spin-down conductance $\mathcal{G}_\downarrow$ (dashed line) each as a function of the magnetic flux phase ϕ for different values of Γ, t_j, and φ with $\varepsilon_j=0$, $\varepsilon_\mathrm{F}=0$; (b) spin-polarized conductance as a function of the magnetic flux phase ϕ for different Rashba SOI phase $\varphi=0.25\pi$, 0.5π.

For the case of tuning all QD energy levels $\varepsilon_j=\varepsilon_0$ fluctuating of Fermi energy level $\varepsilon_\mathrm{F}=0$ by adjusting gate voltage in experiment, figure 3 shows the spin polarization of the linear conductance is enhanced by increasing the inter-dot coupling strength t_j for the best matching of $\varphi=\pi/2$ and $\phi=\pi/2$ and lead-dot coupling strength $\Gamma=t_0$. When the intra-dot Coulomb repulsion U_j is far less than inter-dot coupling, we can leave out the on-site Coulomb repulsion effect by assuming $U_j=0$. The spin polarization does not exist at all for the vanishing inter-dot coupling strength at $t_j=0$, and there appears an identical Breit–Wigner lineshape in the conductance spectrum for each of $\mathcal{G}_\uparrow$ and $\mathcal{G}_\downarrow$ as shown in Fig. 3(a), and its corresponding spin polarization p is shown in Fig. 4(c) (solid line). The resonance-peaks of $\mathcal{G}_\uparrow$ exhibit opposite direction compared with those of $\mathcal{G}_\downarrow$ by increasing inter-dot coupling strength t_j (see Figs. 3(b)–3(d)), and the corresponding spin polarization is shown in Fig. 4(c). The complete spin polarization can be obtained when t_j is strong enough, so that $\mathcal{G}_\downarrow$ reaches a maximum and $\mathcal{G}_\uparrow$ vanishes simultaneously. We also investigate the spin polarizations influenced by different values of lead-dot coupling strength Γ with $t_j=t_0$ as shown in Fig. 4(d). The spin polarization is reduced by increasing lead-

dot coupling strength. So, the polarization of linear conductance can be induced by adjusting inter-dot and lead-dot coupling strength t_j and Γ respectively. In particular, the complete spin polarization can be obtained when $\varepsilon_0 = \varepsilon_F = 0$.

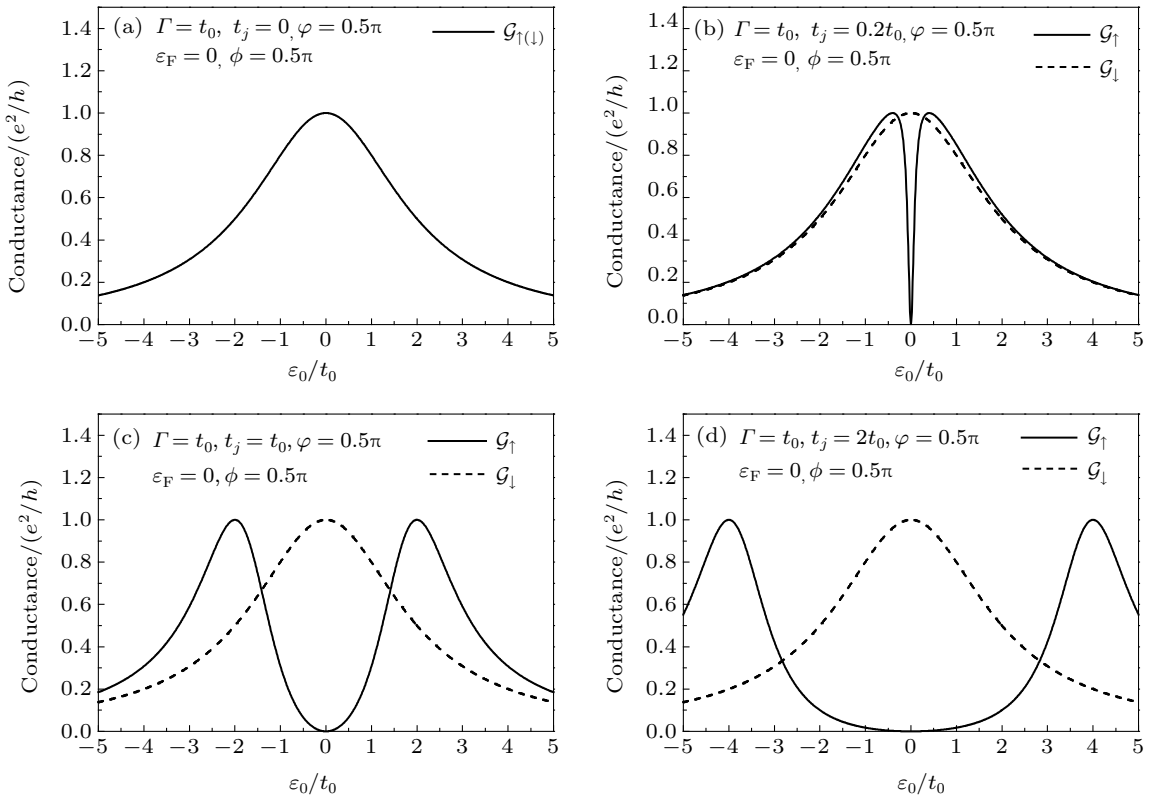


Fig. 3. Curves of spin-polarized conductance versus QD level ε_0 for different values of inter-dot coupling strength t_j: (a) 0, (b) $0.2t_0$, (c) t_0, and (d) $2t_0$.

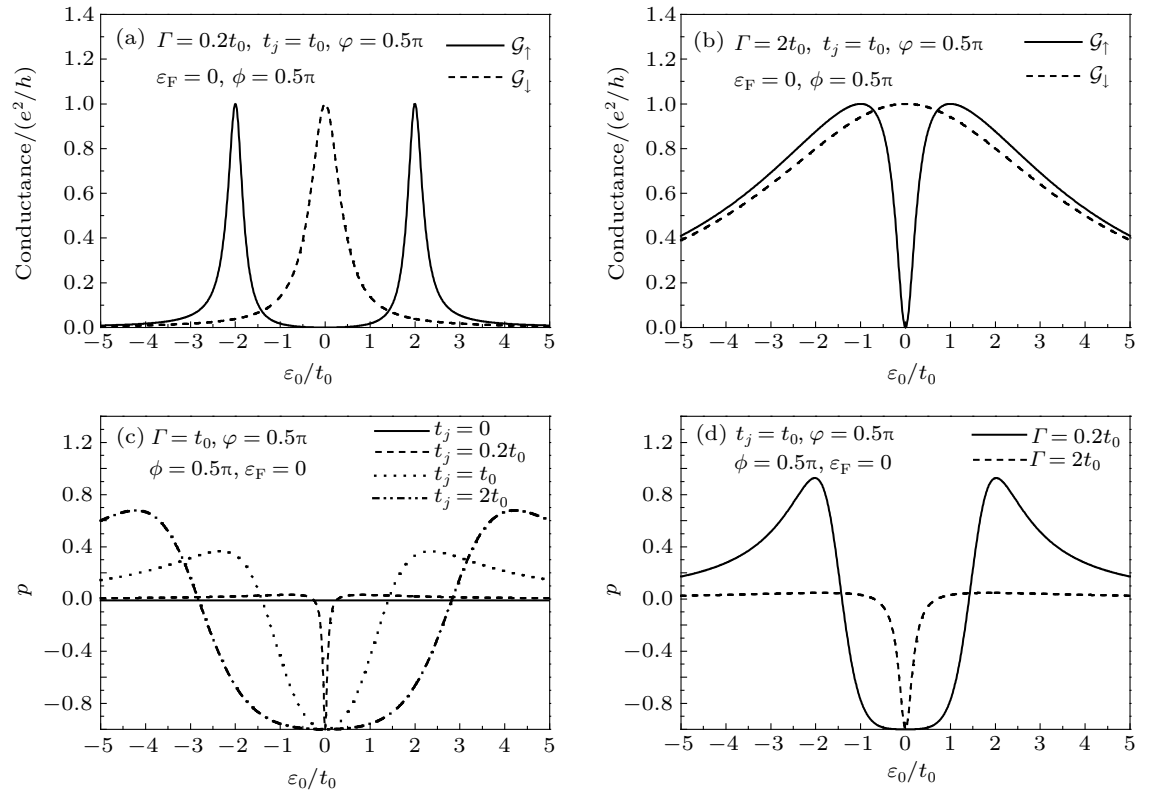


Fig. 4. Curves of polarized conductance versus QD level ε_0 at lead-dot coupling strength $\Gamma = 0.2t_0$ (a) and $\Gamma = 2t_0$ (b), and curves of spin polarization p versus QD level ε_0 at lead-dot coupling strength $\Gamma = t_0$ (c) where the spin polarization is corresponding to that in Fig. 3, and $\Gamma = 0.2t_0$, $2t_0$ (d) where the spin polarizations are corresponding to those in Figs. 4(a) and 4(b).

Such a result can be analyzed in the molecular orbital representation. It is well known that the linear conductance spectrum of the coupled QD structure reflects the eigenenergy spectrum of the molecule made up of the coupled QDs. When we adopt the parameter values as those in Fig. 3, we can obtain both spin-up and spin-down eigenenergies of the QD molecule by the molecular eigenenergy formula $e_m = \varepsilon_j + 2t_j\cos(m\pi/2)$ in Section 3, with the values of $e_1 = e_3 = \varepsilon_0$, $e_2 = \varepsilon_0 - 2t_0$, and $e_4 = \varepsilon_0 + 2t_0$, where e_1 and e_3 are degenerate eigenenergies because of the symmetry of the geometric configuration of the coupled QD ring. In particular, all molecular eigenenergies are shown to be degenerate since $e_1 = e_2 = e_3 = e_4 = \varepsilon_0$ when $t_j = 0$, which induces the spin-up and spin-down electrons to have the same transport properties. So, no spin polarized phenomenon appears as shown in Fig. 3(a). From the other panels in Fig. 3, we find that two resonance peaks exist in the $\mathcal{G}_\uparrow$ conductance spectrum, corresponding to the points of $e_2 = \varepsilon_0 - 2t_0 = \varepsilon_F$ or $e_4 = \varepsilon_0 + 2t_0 = \varepsilon_F$, moreover, an antiresonance point appears at the position of $e_1 = e_3 = \varepsilon_0 = \varepsilon_F$, which arises from the destructive interference among electron waves passing through the molecular orbits. Also by Eq. (17), $\gamma^{\alpha}_{11,\uparrow} = 0$ or $\gamma^{\alpha}_{33,\uparrow} = 0$ can be obtained with $\varphi = \pi/2$ and $\phi = \pi/2$, so it is suggested that the degenerate molecular states $|1,\uparrow\rangle$ and $|3,\uparrow\rangle$ are completely decoupled from the leads and become bound states. However, only one resonance peak corresponds to the position of $\varepsilon_0 = e_1 = e_3 = \varepsilon_F$ and the conductance spectrum presents a Breit–Wigner lineshape for the $\mathcal{G}_\downarrow$ conductance. Obviously, there exist different decoupled molecular states from those for $\mathcal{G}_\uparrow$ conductance spectrum. By Eq. (17), we can easily obtain $\gamma^{\alpha}_{22,\downarrow} = 0$ or $\gamma^{\alpha}_{44,\downarrow} = 0$, which induces the molecular eigenenergy states $|2,\downarrow\rangle$ and $|4,\downarrow\rangle$ to be completely decoupled from the leads and become bound states. Thus, we conclude that adjusting the phase factor of Rashba SOI and the magnetic flux is the fundamental reason for inducing the spin polarization phenomenon by the different molecular states of the different spin electrons completely decoupled from the leads and giving rise to BIC in the symmetric coupled QD structure. Furthermore, t_j and Γ are the significant factors to modify behavior of the spin polarization, due to the molecular eigenenergies and $\gamma^{\alpha}_{mm,\sigma}$ dependent on t_j and Γ, respectively. In a word, the positions or the linewidth of the conductance peaks can be controlled only by gate voltage.

Next, we pay attention to the effect of the electron interaction on the spin-dependent conductance spectrum. Usually, the electron interaction is prominent only by considering the intra-dot Coulomb repulsion, i.e., the Hubbard term. It is known that the Coulomb interaction plays an important role in electron transport through the coupled-QD structure,[30–34] for the reason that the quantum interference is modified by the Coulomb-induced energy level splitting of the QD levels. Then, the Coulomb-induced multi-channel quantum interference presents some complicated properties quite different from those in the noninteracting case. In Fig. 5, we investigate the Coulomb-modified linear conductance spectra each as a function of ε_0 and the average electron number in QDs under the assumption of uniform Coulomb repulsion $U_j = U = 2t_0$. It can be found that the spin polarization still exists in the conductance spectrum and both the spin-up and spin-down conductances split into two groups due to the Coulomb-induced splitting of the QD levels. Between the two separated groups there is an antiresonance fixed in the conductance spectrum. Note that in contrast to the conventional electron–hole symmetry, the position of such a conductance zero deviates from $\varepsilon_0 = -U/2$. We can readily explain this phenomenon by the fact that the decoupling states occur in the system, the average electron occupation number $\langle n_{j\sigma}\rangle$ is no longer equal to $1/2$ (see Fig. 5(b)), and the electron–hole symmetry is broken.[22,23]

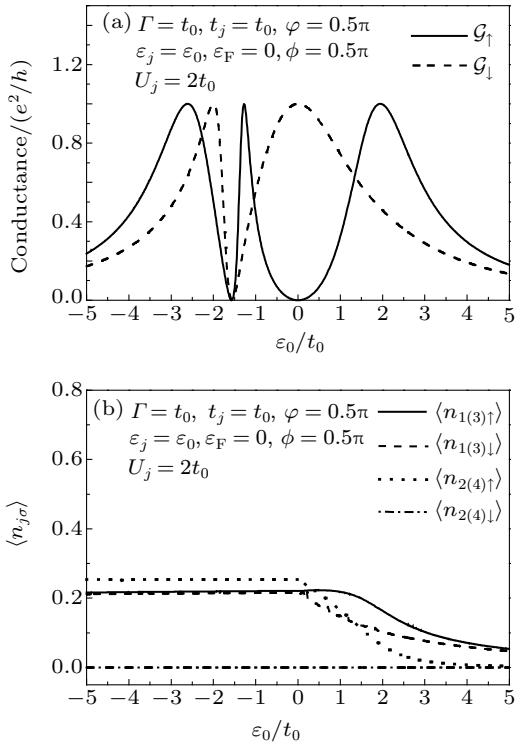


Fig. 5. (a) Curves of spin-polarized conductance versus QD level ε_0 at Coulomb interaction strength $U_j = 2t_0$, and (b) curves of average electron occupation number $\langle n_{j\sigma}\rangle$ versus QD level ε_0.

In addition, in the right group of the $\mathcal{G}_\uparrow$ conductance spectrum, the exhibitions of decoupled molecular states and antiresonance are similar to those in the absence of Coulomb interaction, due to the molecular state $|4,\uparrow\rangle$ adjusting the QD level higher than the Fermi level ε_F of the system. It indicates that the average electron occupation number $\langle n_{4\downarrow}\rangle$ is almost zero as shown in Fig. 5(b) and the Coulomb-induced splitting of the QD levels does not happen, and then the resonance peak appears at $\varepsilon_0 = -2.00t_0$. The other molecular state $|2,\uparrow\rangle$ is split into two peaks at $\varepsilon_0 = -1.30t_0$ and $\varepsilon_0 = -2.70t_0$, respectively, from the original position of $e_2 = \varepsilon_0 - 2t_0 = \varepsilon_F$. The antiresonance between the two peaks can be determined by expression (18). When $\phi = \pi/2$, $\varphi = \pi/2$, and $\sigma = \uparrow$, we can

obtain

$$T_{\mathrm{LR},\uparrow} = \frac{4\Gamma_0^2(z-\varepsilon_0-U+U\langle n_{1\downarrow}\rangle)^2}{(z-\varepsilon_0)^2(z-\varepsilon_0-U)^2+4\Gamma_0^2(z-\varepsilon_0-U+U\langle n_{1\downarrow}\rangle)^2}\,. \quad (19)$$

The antiresonance position $\varepsilon_0 = -(1-\langle n_{1\downarrow}\rangle)U = -1.58t_0$ is given by $T_{\mathrm{LR},\uparrow}(\varepsilon_{\mathrm{F}}) = 0$ with $\varepsilon_{\mathrm{F}} = 0$, $z = \varepsilon_{\mathrm{F}} + \mathrm{i}0^{+}$, $\varepsilon_0 = z - U + U\langle n_{1\downarrow}\rangle = -(1-\langle n_{1\downarrow}\rangle)U$, and $\langle n_{1\downarrow}\rangle = 0.21$ as shown in Fig. 5(b). In this sense we see that the many-body effect can influence the spin polarization to some extent and the occurrence of decoupling states causes the electron–hole symmetry to be broken. However, the many-body effect does not modify the behavior of the spin polarization at the point of Fermi energy.

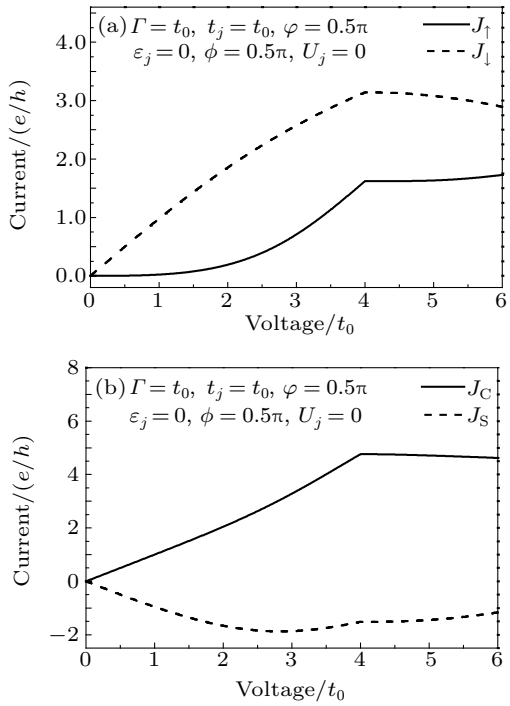


Fig. 6. Curves of current versus finite bias voltage with the same parameters as those in Fig. 3(c).

Finally, we come to investigate the J–v characteristics of this structure in order to further clarify the behavior of the electron-spin polarization transport induced by Rashba SOI. The corresponding numerical results are shown in Fig. 6 and Fig. 7. In Fig. 6(a), the spin-up and spin-down currents versus the finite bias voltage are plotted. They show that with the adjustment of the bias voltage the properties of spin-dependent current are still robust in such a structure. The spin-down current occupies a dominant position because of its value being larger than the spin-up one. When the bias voltage is between 0 and t_0, the spin-up current is zero, which means that the spin-up electron is repressed through this structure, and only the spin-down electron can be transported. So we can see that in the case of low voltage, the filtration of the spin-down current can be realized from this structure with the corresponding parameters. Moreover, in Fig. 7(a) a more interesting phenomenon appears in that in the whole range of voltage we investigate, the spin-up current is entirely restrained by tuning the structure parameters with the weak QD-lead coupling strength $\Gamma = 0.1t_0$ and the strong inter-dot coupling strength $t_j = 2t_0$. From the definitions of the charge current J_{C} and the spin current J_{S}, we can easily understand the numerical results as shown in Figs. 6(b) and 7(b). They show that in such a structure applying a finite bias voltage between the leads can efficiently bring out pure spin current with opposite charge current. Furthermore, by comparing Fig. 6(b) and Fig. 7(b), we can find that the value of spin current is coincident with the charge current by adjusting the structure parameters. Thus we can realize the pure spin current transport through such a structure.

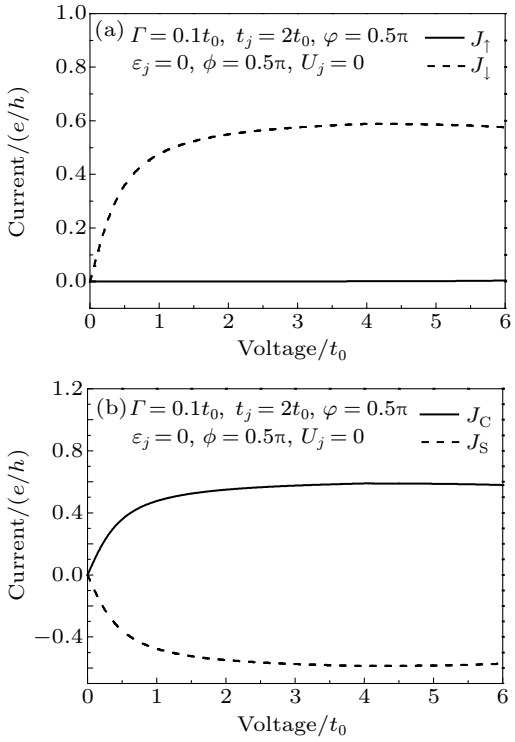


Fig. 7. Curves of current versus finite bias voltage with $\Gamma = 0.1t_0$ and $t_j = 2t_0$.

5. Summary

In this work we systematically studied the spin-polarized phenomenon in the electron transport process through a four-QD AB ring, by introducing a local Rashba spin–orbit interaction to an individual QD-1. First, it is found that the spin-polarized linear conductance is a periodic function of ϕ with a period of 2π, so we can fully control the complete spin polarization at zero bias voltage by introducing Rashba phase φ and adjusting magnetic flux phase ϕ. Then, in the case of $\varphi = \phi = \pi/2$, the appearance of spin polarization is reduced by the different molecular states of the different spin electron completely decoupled from the leads, and the degree of spin polarization is mainly influenced by two structure factors: inter-dot and lead-dot coupling strengths, t_j and Γ. This characteristic is useful to make a qubit. Besides, when the many-body effect is taken into account, the Coulomb-induced multi-channel quantum interference presents some complicated properties quite different from those in the noninteracting case and the electron–hole symmetry is broken. Finally,

we can efficiently control the directions of the pure spin currents through such a structure by adjusting a finite bias on the leads. Such a result is helpful for designing a spin current filter. We hope that all these results could be helpful for relevant experiments.

References

[1] Zutic I, Fabian J and Sarma S D 2004 *Rev. Mod. Phys.* **76** 323
[2] Wang B, Wang J and Guo H 2003 *Phys. Rev. B* **67** 092408
[3] Dong B, Cui H L and Lei X L 2005 *Phys. Rev. Lett.* **94** 066601
[4] Tang C S, Mal'shukov A G and Chao K A 2005 *Phys. Rev. B* **71** 195314
[5] Sun Q F, Xie X C and Wang J 2008 *Phys. Rev. B* **77** 035327
[6] Chen K W and Chang C R 2008 *Phys. Rev. B* **78** 235319
[7] Wang S X, Yuan A G and Du J 2010 *Acta Phys. Sin.* **59** 2760 (in Chinese)
[8] Wang S X, Du J and Yuan A G 2010 *Acta Phys. Sin.* **59** 2767 (in Chinese)
[9] Xiong S J and Liu P 2009 *Chin. Phys. B* **18** 5414
[10] Sun Q F, Wang J and Guo H 2005 *Phys. Rev. B* **71** 165310
[11] Lu H F and Gou Y 2007 *Phys. Rev. B* **76** 045120
[12] Rashba E I 1960 *Sov. Phys. Solid State* **2** 1109
[13] Bychkov Y A and Rashba E I 1984 *J. Phys. C* **17** 6039
[14] Li B X and Chi F 2009 *Superlatt. Microstrucut.* **45** 39
[15] Li S S and Xia J B 2008 *Appl. Phys. Lett.* **92** 022102
[16] Chi F and Li S S 2006 *J. Appl. Phys.* **100** 113703
[17] Lü H F and Guo Y 2007 *Appl. Phys. Lett.* **91** 092128
[18] Chi F and Zheng J 2008 *Appl. Phys. Lett.* **92** 062106
[19] Chi F, Zheng J and Sun L L 2008 *Appl. Phys. Lett.* **92** 172104
[20] Han Y, Gong W J and Wei G Z 2009 *Commun. Theor. Phys.* **52** 1117
[21] Han Y, Gong W J and Wei G Z 2009 *Phys. Status Solidi B* **246** 2140
[22] Han Y, Gong W J and Wei G Z 2009 *Phys. Status Solidi B* **246** 1634
[23] Wu L J, Han Y, Gong W J and Tan T Y 2011 *Acta Phys. Sin.* **60** 107303 (in Chinese)
[24] Gong W, Han Y and Wei G 2009 *Solid State Commun.* **149** 1831
[25] Jouho A P, Wingreen N S and Meir Y 1994 *Phys. Rev. B* **50** 5528
[26] Meir Y and Wingreen N S 1992 *Phys. Rev. Lett.* **68** 2512
[27] Wingreen N S and Meir Y 1994 *Phys. Rev. B* **49** 11040
[28] Gong W J, Zheng Y, Liu Y and Lü T 2006 *Phys. Rev. B* **73** 245329
[29] Heary R J, Han J E and Zhu L 2008 *Phys. Rev. B* **77** 115132
[30] Bulka B R and Stefański P 2001 *Phys. Rev. Lett.* **86** 5128
[31] Hofstetter W, König J and Schhoeller H 2001 *Phys. Rev. Lett.* **87** 156803
[32] Ding G H, Kim C K and Nahm K 2005 *Phys. Rev. B* **71** 205313
[33] Karrasch C, Enss T and Meden V 2006 *Phys. Rev. B* **73** 235337
[34] Gong W J, Han Y, Xie X F and Wei G Z 2010 *Phys. Status Solidi B* **247** 2222